JOURNAL OF CATALYSIS 122, 280–294 (1990)

Structure Sensitivity of Methane Oxidation over Platinum and Palladium

ROBERT F. HICKS,[1] HAIHUA QI,[2] MICHAEL L. YOUNG, AND RAYMOND G. LEE

Chemical Engineering Department, 5531 Boelter Hall, University of California, Los Angeles, California 90024-1592

Received June 22, 1989; revised September 14, 1989

A series of supported platinum and palladium catalysts were tested for methane oxidation at 260 to 370°C, 50 Torr methane, 110 Torr oxygen, 900 Torr helium, and conversions below 2%. The intrinsic rate varies by more than 5000 from the least active to the most active catalyst, indicating that the reaction is structure sensitive. The catalytic activity of platinum depends on the distribution of the metal between a dispersed and a crystalline phase. These two phases are distinguished by absorbances at 2068 and 2080 cm^{-1}, respectively, in the infrared spectrum of adsorbed carbon monoxide. The catalytic activity of palladium depends on the metal particle size. For the different classes of catalysts, the mean steady state turnover frequency (TOF) at 335°C and the mean apparent activation energy (E_a) are as follows: dispersed phase of platinum, TOF = 0.005 s^{-1} and E_a = 36 kcal/mole; crystalline phase of platinum, TOF = 0.08 s^{-1} and E_a = 28 kcal/mole; small particles of palladium, TOF = 0.02 s^{-1} and E_a = 27 kcal/mole; and large particles of palladium, TOF = 1.3 s^{-1} and E_a = 29 kcal/mole. The structure sensitivity may be explained by differences in the reactivity of the adsorbed oxygen on these metal surfaces.

INTRODUCTION

Catalysts play an important role in reducing emissions from hydrocarbon combustion processes. They have been used two ways: as an additive to the combustor to enhance heterogeneous reactions (*1–5*), or as an emissions control device located downstream of the combustor (*6–9*). The advantage of a catalytically enhanced combustor is that it operates at much lower temperatures than an open flame burner, and greatly reduces the emissions of nitrogen oxides. However, the thermal stability of the catalyst is a limiting factor in this application.

Several studies of methane oxidation over platinum and palladium have been reported (*4, 10–17*). These were motivated by the observation that methane is a large component of the hydrocarbon emissions from combustion processes and that it is the most difficult hydrocarbon to oxidize. Moreover, there is a direct application of the results to the catalytic combustion of natural gas (*4*). Most of the prior work has been concerned with the kinetics and mechanism of this reaction. Several studies examined the effect of catalyst composition on the rate (*10, 13–16*). However, in only one case (*14*) has the effect of catalyst structure been considered.

We have undertaken a study to characterize the effects of catalyst structure on the intrinsic activity of platinum and palladium for methane oxidation. In this paper, we provide a comparison of the turnover frequencies observed over platinum and palladium under a standard set of reaction conditions. Several different aluminas and zirconias have been used as catalyst supports. The metal dispersions vary over a range sufficient to give large changes in the distribution of sites on the crystallite surfaces (*18*). The morphology of the crystallites is qualitatively assessed by infrared spectroscopy of adsorbed carbon monoxide. In the accompanying paper, we exam-

[1] To whom correspondence should be addressed.

[2] Current address: Chemistry Department, Nanjing University, Nanjing, China.

0021-9517/90 $3.00

TABLE 1

Recipes for Preparation of the Catalysts

Sample number	Support composition	Support calcined 48 hr in air (°C)	Support surface area (m^2/g)	Metal salt	Deposition technique	Catalyst calcined 2 hr in air (°C)	Metal weight loading (%)
1	α-AlOOH(A)[a]	No	160	H_2PtCl_6	Ion exchange	500	0.80
2	α-AlOOH(A)	1050	60	$Pt(NH_3)_4Cl_2$	Impregnation[b]	500	0.50
3b	Al_2O_3(D)[c]	1000	83	H_2PtCl_6	Ion exchange	500	0.84
4	ZrO_2(D)	1000	83	H_2PtCl_6	Ion exchange	700	0.78
5	ZrO_2(Z)[d]	No	42	$Pt(NH_3)_4Cl_2$	Ion exchange	500	0.30
6	12% Y_2O_3/ZrO_2(Z)	1050	3	H_2PtCl_6	Impregnation	500	0.50
7	12% Y_2O_3/ZrO_2(Z)	1050	3	H_2PtCl_6	Impregnation	500	0.50
8	α-AlOOH(A)	1050	3	$Pt(NH_3)_4Cl_2$	Impregnation	500	0.50
9	α-AlOOH(A)	1050	60	H_2PdCl_4	Impregnation	500	0.50
10	α-AlOOH(A)	1200[e]	4	$Pd(NH_3)_4Cl_2$	Impregnation	500	0.50
11b	Al_2O_3(D)	1200[e]	4	$Pd(NH_3)_4Cl_2$	Impregnation	500	2.00
12a	Al_2O_3(D)	1000	83	H_2PdCl_4	Ion exchange	700	0.20
12b	Al_2O_3(D)	1000	83	H_2PdCl_4	Ion exchange	500	0.46
13b	Al_2O_3(D)	1000	83	H_2PdCl_4	Ion exchange	700	0.46
14	12% Y_2O_3/ZrO_2(Z)	1000	83	H_2PdCl_4	Ion exchange	700	2.30
		1050	3	H_2PdCl_4	Impregnation	500	0.50

[a] A = Alpha products; α-AlOOH dehydrates to Al_2O_3 when heated above 450°C.
[b] Incipient wetness impregnation.
[c] D = Degussa flame-synthesized metal oxides.
[d] Z = Zircar precipitated metal oxides.
[e] Calcined in air 2 hr only.

ine in greater detail the effect of catalyst structure on methane oxidation over palladium supported on alumina (*19*).

METHODS

The catalyst supports used in this study were Alpha Products AlOOH, Degussa flame-synthesized Al_2O_3 "C", Degussa flame-synthesized ZrO_2, Zircar precipitated ZrO_2, and Zircar precipitated 12 mol% Y_2O_3/ZrO_2. The AlOOH decomposed to Al_2O_3 upon heating in air at 450°C. The surface area of AlOOH decreased continuously from 160 to 60 m^2/g during heating for 2-h intervals at temperatures from 500 to 1000°C. The Degussa and Zircar zirconias had initial surface areas between 30 and 45 m^2/g. These surface areas could be maintained during heating in air at temperatures up to 700°C. However, they rapidly decreased during further heating, and at 1000°C, the surface areas fell to about 3 m^2/g. The support with the highest thermal stability was the Degussa Al_2O_3. Its surface area remained constant at 83 m^2/g during heating in air for 2 to 48 h at 1000°C. Most of the supports were calcined prior to depositing the precious metals on them.

Recipes used to prepare the catalyst samples are summarized in Table 1. The metals were deposited by ion exchange or by incipient wetness impregnation (*20*). The acidic chloride and the basic amine dichloride complexes were used. After adsorption of the metal salts onto the supports, the catalyst were dried at 105°C overnight and then calcined in air for 2 h at either 500 or 700°C. Samples removed from the oven were immediately stored in a desiccator. The metal weight loadings of the calcined catalysts were determined by inductively coupled plasma emission spectroscopy.

The metal dispersion (surface atoms/total atoms) of each sample was determined by volumetric chemisorption (*20*). From 1 to 3 g of catalyst was pelletized, crushed, and sieved to 32–60 mesh. The pellets were placed in a quartz chamber, reduced in 200 cm^3/min hydrogen for 1 h at 300°C, and then cooled to 25°C in 5×10^{-7} Torr vacuum (1 Torr = 133 N/m^2). At room temperature, adsorption isotherms were measured in the pressure range 10 to 150 Torr. The linear dependency of the gas uptake on pressure at the higher pressures was back-extrapolated to zero to give the amount chemisorbed. The exposed platinum was determined by hydrogen titration of preadsorbed oxygen, assuming a reaction stoichiometry of 1.5 $H_2/Pt–O_s$ (*21*). The exposed palladium was determined by carbon monoxide adsorption, assuming a reaction stoichiometry of 1.06 CO/Pd_s (*22*).

The intrinsic rates of methane oxidation were determined in a fixed-bed microreactor. Between 0.05 and 0.2 g of catalyst pellets was loaded into a 6.35-mm-o.d. quartz tube, and the tube mounted inside a forced-air, tubular furnace. The catalyst temperature was measured by a thermocouple placed just upstream of the bed. Reactor effluent was analyzed by an on-line gas chromatograph, equipped with 1.83-m Carbosphere packed column and thermal conductivity detector. Carbon dioxide was the only reaction product observed.

Rate measurements were carried out as follows. The sample was heated in 50 cm^3/min helium to 300°C, and reduced in 50 cm^3/min hydrogen for 1 h at 300°C. The bed temperature was then adjusted to the reaction temperature in flowing helium. Next, the reaction was started by introducing 50 Torr methane, 110 Torr oxygen, and 900 Torr helium at flow rates between 200 and 760 cm^3/min (STP). The reaction was continued until a steady state rate was obtained. This time varied from 4 to 20 h. At steady state, apparent activation energies were determined by varying the temperature ±15°C about the mean. The mean temperature during a run ranged from 350 to 370°C for the platinum catalysts and from 260 to 350°C for the palladium catalysts. The amount of catalyst used, the flow rates, and the temperatures were selected to keep the methane conversion between 0.2 and 2.0%. Below 2% conversion, the concentration of carbon dioxide in the gas leaving the reactor followed a linear dependence on the inverse of the total flow rate, thus ensuring no mass transport disguise of the rate.

Infrared spectra of adsorbed carbon monoxide were obtained in an evacuable glass cell. A 0.1-g sample of catalyst was pressed into a 13-mm-diameter wafer and placed in the cell. The wafer was pretreated as described above in the chemisorption experiment. At room temperature, small aliquots of carbon monoxide, 0.5 to 2.5×10^{-7} mole, were dosed into the chamber and the infrared spectrum was recorded. The intensity of the bands for adsorbed carbon monoxide increased linearly with each dose until the saturation point was reached (*22*). The spectra shown in this report are for saturation only. The infrared spectra were recorded on a Digilab FTS-40 spectrometer with a DTGS detector at 4 cm^{-1} resolution and coadding 256 scans.

RESULTS

Activities of the Platinum Catalysts

The effect of reaction time on the turnover frequencies for methane oxidation over eight platinum catalysts is shown in Table 2. The turnover frequencies are based on the moles of carbon dioxide formed per second per mole of surface platinum atoms present initially. A variety of time-dependent behaviors are exhibited by the catalysts. Samples, 1, 2, 6, and 7 exhibit 1-h induction periods in which the rates rise from zero to a steady value. Samples 3b, 4, and 5 exhibit high initial rates which decline gradually throughout the run. Sample 3a is peculiar in that the rate of methane oxidation over this catalyst increases steadily

TABLE 2

Effect of Time on the Turnover Frequency for Methane Oxidation over Platinum

Sample number	Mean reaction temperature (°C)	Turnover frequency (s^{-1}) at 370°C[a]						
		Initial	1 hr	2 hr	4 hr	6 hr	8 hr	Final (time (hr))
1	370	n.d.[b]	0.007	0.007	0.007	0.007	0.007	0.007 (12)
2	350	0.08	0.30	0.35	0.38	0.38	0.36	0.36 (12)
3a	370	0.005	0.007	0.008	0.011	0.017	0.019	0.024 (17)
3b	370	0.08	0.06	0.05	0.04	—	—	0.04 (4)
4	350	0.65	0.32	0.28	0.23	0.21	—	0.21 (6)
5	350	0.29	0.36	0.32	0.27	0.25	0.23	0.23 (8)
6	370	n.d.	0.08	0.16	0.22	0.16	—	0.18 (7)
7	350	n.d.	0.29	0.33	0.35	0.37	0.35	0.35 (8)

[a] Corrected to 370°C using the measured activation energies.
[b] n.d. = no CO_2 detected.

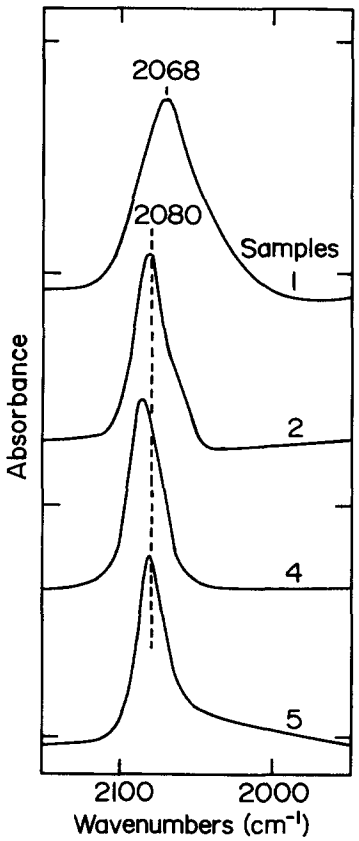

FIG. 1. Infrared spectra of adsorbed carbon monoxide at saturation coverage on platinum catalyst samples 1, 2, 4, and 5. Infrared spectra were recorded before exposure to reaction conditions.

during the 17-h run and never attains a constant value. Examination of the turnover frequencies measured at the end of the run reveals that they vary over a wide range, from 0.007 s^{-1} for sample 1 to 0.36 s^{-1} for sample 2.

Infrared spectra of carbon monoxide adsorbed at saturation coverage on samples 1, 2, 3a, 3b, 4, and 5 are shown in Figs. 1 and 2. Also shown in Fig. 2 is the infrared spectrum of carbon monoxide adsorbed on samples 3a and 3b after exposure to reaction conditions. All samples, including those which had been exposed to reaction conditions, were reduced at 300°C prior to adsorbing the carbon monoxide. The infrared bands range in frequency from 2065 to 2083 cm^{-1}, and may be ascribed to linearly bonded carbon monoxide (*23–26*). Not shown is a very small absorbance at about 1850 cm^{-1}, which is due to bridge-bonded carbon monoxide.

There are notable differences in the infrared spectra. For samples 2, 4, and 5, the infrared peak is narrow and centered at 2080 cm^{-1}. Conversely, for samples 1, 3a, and 3b, the infrared peak is broad and centered at 2068 cm^{-1}. Samples 3a and 3b exhibit a high-frequency shoulder on the main peak. After exposure to reaction condi-

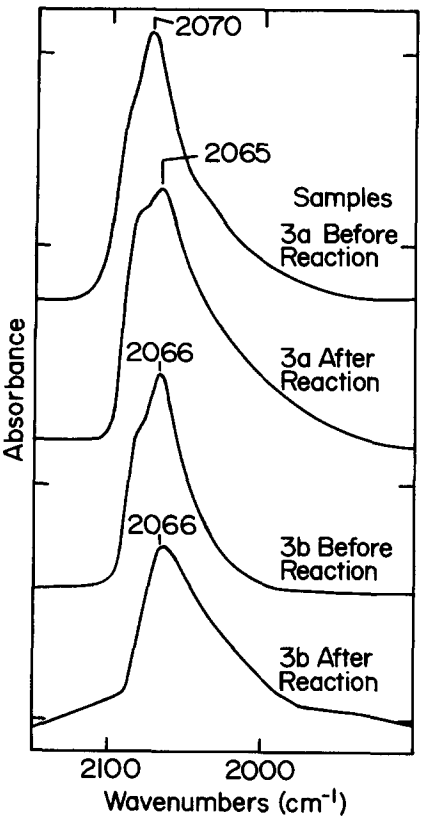

FIG. 2. Infrared spectra of adsorbed carbon monoxide at saturation coverage on platinum catalyst samples 3a and 3b. The infrared spectra were recorded before and after exposure to reaction conditions.

tions, the shoulder increases for sample 3a, while it decreases for sample 3b.

The physical properties of the platinum catalysts are compared to the turnover frequencies and the activation energies for methane oxidation in Table 3. The dispersions and the infrared results shown are for the fresh samples. Turnover frequencies extrapolated to zero time differ little from those recorded at the end of the run. There are basically two sets of catalyst samples: those of low activity, numbers 1, 3a, and 3b; and those of high activity, numbers 2, 4, 5, 6, and 7. Activation energies are significantly higher on samples of low activity than on those of high activity. No correlation of the dispersion with turnover frequency is observed. For example, samples 3a and 4 both have high dispersions, yet one of the samples exhibits low activity while the other exhibits high activity. On the other hand, the infrared bands for adsorbed carbon monoxide clearly correlate with turnover frequencies. Samples showing a broad infrared peak located at 2068 cm^{-1} give low rates of methane oxidation. Conversely, samples showing a narrow infrared peak located at 2080 cm^{-1} give high rates of methane oxidation.

For samples 3a and 3b, there is also a correlation of before and after infrared spectra with the changes in turnover rate observed during the run. The activity of sample 3a increased steadily during reaction, and this was accompanied by an increase in the high-frequency shoulder of the infrared peak at approximately 2080 cm^{-1}. By comparison, the activity of sample 3b decreased during reaction, and this was accompanied by a decrease in the high-frequency shoulder. These trends are consistent with the results observed for the different catalyst samples; namely, high reaction rates correspond to the 2080 cm^{-1} peak, while low reaction rates correspond to the 2068 cm^{-1} peak.

Activities of the Palladium Catalysts

The effect of reaction time on the turnover frequencies of eight palladium catalysts is shown in Table 4. The turnover frequency is based on the moles of carbon dioxide produced per second per mole of surface palladium atoms present initially. As was observed for platinum, the palladium catalysts exhibit a variety of time-dependent behaviors. Sample 10 exhibits a 1-h induction period, after which a high but gradually declining rate is established. Sample 11b has a relatively low initial activity, which declines by half over the first hour of reaction, and remains constant thereafter. Samples 8, 9, 12b, 13b, and 14

TABLE 3

Effect of Catalyst Structure on the Activity of Platinum for Methane Oxidation

Sample number	Catalyst composition	Initial dispersion (%)	Initial carbon monoxide IR absorbance		Turnover frequency (s^{-1}) at 335°C		Activation energy (kcal/mole)[c]
			Frequency (cm^{-1})	FWHM[a] (cm^{-1})	Initial[b]	Final	
1	0.8% Pt/Al_2O_3	67	2068	46	0.001	0.001	39.3
3a	0.84% Pt/Al_2O_3	90	2070	43	0.001	0.005	33.6
3b	0.78% Pt/Al_2O_3	6	2066	38	0.02	0.01	33.0[d]
2	0.5% Pt/Al_2O_3	31	2077	24	0.10	0.10	29.0
4	0.3% Pt/ZrO_2	100	2083	24	0.07	0.05	32.4
5	0.5% Pt/ZrO_2	40	2081	21	0.09	0.06	27.6
6	0.5% $Pt/YZrO_2$	30	—	—	0.06	0.06	26.6
7	0.5% $Pt/YZrO_2$	20	—	—	0.11	0.11	26.6

[a] Full width at half-maximum of infrared peak.
[b] Initial value obtained by linear extrapolation of data at 2–17 hr of reaction back to zero time.
[c] 1 kcal = 4.184 kJ.
[d] Assumed value based on the activation energies measured for the other samples.

exhibit 4- to 8-h induction periods in which the rate gradually increases to a constant value. Sample 12a also exhibits a gradually increasing rate; however, in this case, no leveling off of the rate was noticeable at the end of the 8-h run. This long induction period is a feature of the palladium catalysts which is distinctly different from the trends observed for the platinum catalysts. The turnover frequencies measured at the end of the run vary over a wide range for the eight samples, from 0.005 s^{-1} for sample 11b to 1.24 s^{-1} for sample 10.

Shown in Figs. 3 and 4 are infrared spectra of adsorbed carbon monoxide on the palladium catalysts after exposure to reac-

TABLE 4

Effect of Time on the Turnover Frequency for Methane Oxidation over Palladium

Sample number	Mean reaction temperature (°C)	Turnover frequency (s^{-1}) at 300°C[a]						
		Initial	1 hr	2 hr	4 hr	6 hr	8 hr	Final (time (hr))
8	280	n.d.[b]	0.21	0.29	0.47	0.57	0.50	0.50 (8)
9	300	0.012	0.015	0.15	0.21	0.23	0.32	0.30 (16)
10	280	n.d.	1.68	1.59	1.33	—	—	1.24 (5)
11b	350	0.010	0.005	0.005	0.005	0.005	—	0.005 (7)
12a	310	n.d.	0.001	0.007	0.010	0.012	0.015	0.015 (8)
12b	300	n.d.	0.008	0.009	0.012	0.012	—	0.012 (7)
13b	300	0.027	0.11	0.33	0.86	—	—	0.80 (5)
14	260	n.d.	0.12	0.25	0.65	0.83	1.09	1.00 (13)

[a] Corrected to 300°C using the measured activation energies.
[b] n.d. = no CO_2 detected.

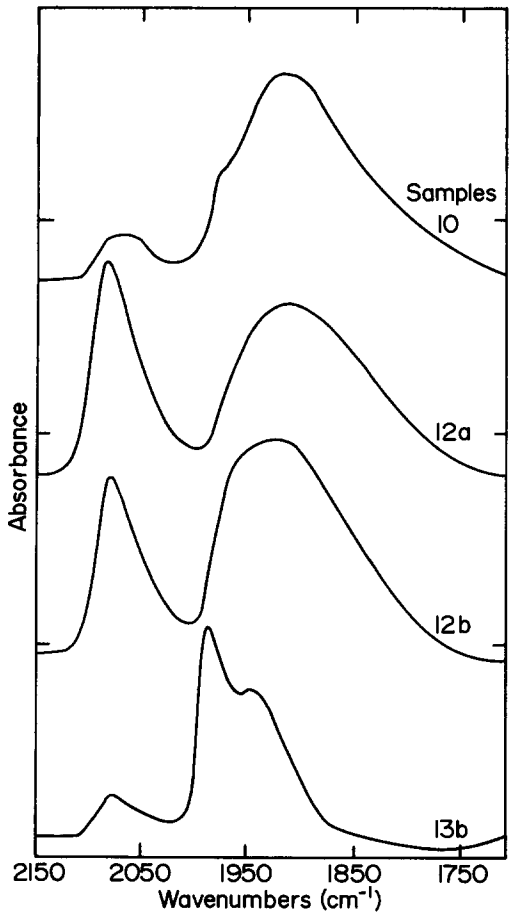

FIG. 3. Infrared spectra of adsorbed carbon monoxide on palladium catalyst samples 10, 12a, 12b, and 13b. The infrared spectra were recorded after exposure to reaction conditions.

tion conditions. Infrared spectra obtained on the fresh catalyst samples are also presented in Fig. 4. Two main bands appear in the spectra, one above and one below 2000 cm^{-1}, which are due to linearly bonded and bridge-bonded carbon monoxide (*22–25*). The broad peak below 2000 cm^{-1} may contain several overlapping absorbances, such as observed for sample 13b. The most prominent distinguishing feature of the infrared spectra is the wide variation in the relative intensities of the bands for linearly bonded and bridge-bonded carbon monoxide.

Three of the catalyst samples, 8, 9, and 11b, underwent large changes in morphology during methane oxidation. This is evident from the redistribution of intensities in the infrared spectra recorded before and after reaction. The spectra for samples 8 and 9 in Fig. 4 reveal a decrease in the peak intensity for linearly bonded carbon monoxide relative to that for bridge-bonded carbon monoxide. In addition, an absorbance at 1970 cm^{-1} becomes more prominent within the low-frequency band. These changes correlate with the large increase in activity observed during reaction over the catalyst samples (see Table 4). The behavior of samples 8 and 9 may be contrasted to that of sample 11b. For sample 11b, the

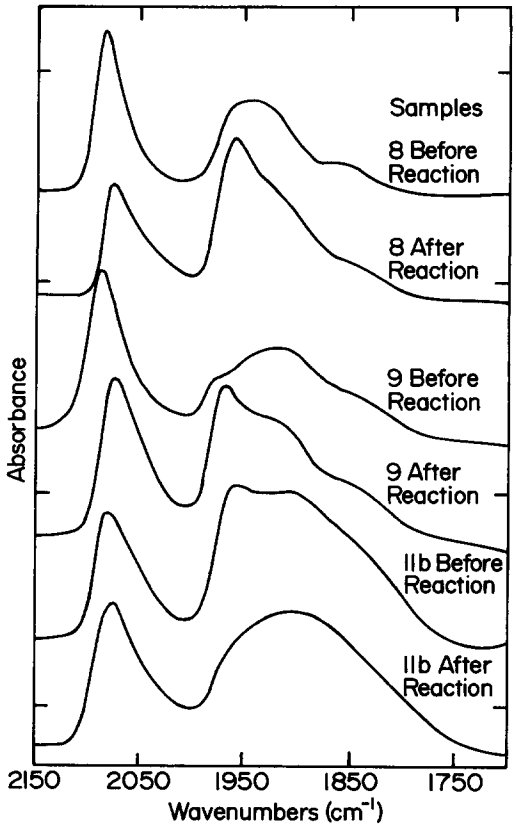

FIG. 4. Infrared spectra of adsorbed carbon monoxide at saturation coverage on palladium catalyst samples 8, 9, and 11b. The infrared spectra were recorded before and after exposure to reaction conditions.

TABLE 5

Effect of Catalyst Structure on the Activity of Palladium for Methane Oxidation

Sample number	Catalyst composition	Initial dispersion (%)	Carbon monoxide IR absorbance, linear/bridge peak ratio[a]		Turnover frequency (s^{-1}) at 335°C[b]	Activation energy (kcal/mole)[c]
			Initial	Final		
11b	0.2% Pd/Al_2O_3	84	0.8	1.1	0.02	25.7
12a	0.46% Pd/Al_2O_3	35	0.8	1.3	0.06	28.2
12b	0.46% Pd/Al_2O_3	56	1.0	0.8	0.05	28.0[d]
8	0.5% Pd/Al_2O_3	63	1.8	0.7	2.3	30.1
9	0.5% Pd/Al_2O_3	33	1.8	1.1	1.2	27.0
10	2.0% Pd/Al_2O_3	12	0.2	0.2	5.6	29.8
13b	2.3% Pd/Al_2O_3	10	0.3	0.2	3.3	28.0[d]
14	0.5% $Pd/YZrO_2$	9	1.7	0.3	4.0	27.3

[a] Ratio of peak heights.
[b] End of run rate.
[c] 1 kcal/mole = 4.184 kJ.
[d] Assumed value based on the activation energies measured for the other samples.

peak for linearly bonded carbon monoxide grows relative to that for bridged-bonded carbon monoxide, and the intensity at 1970 cm^{-1} decreases. These changes correlate with the decrease in activity to a low value during reaction.

The physical properties of the palladium catalysts are compared to the turnover frequencies and the apparent activation energies for methane oxidation in Table 5. The rates are corrected to a reaction temperature of 335°C. These catalysts may be separated into two groups: samples 11b, 12a, and 12b exhibiting low turnover frequencies, between 0.02 and 0.06 s^{-1}; and samples, 8, 9, 10, 13b, and 14 exhibiting high turnover frequencies, between 1.2 and 5.6 s^{-1}. Catalysts with low activity have a number of common features. They consist of low concentrations of small palladium particles (high dispersion) on 83 m^2/g Degussa γ-alumina. In addition, they show linear-to-bridge peak ratios in the infrared spectrum for adsorbed carbon monoxide of about 1.0. By contrast, three catalysts with high activity, samples 10, 13b, and 14, contain large metal crystallites (low dispersion), and they show linear-to-bridge peak ratios after reaction of about 0.2. These results suggest that the turnover frequency for methane oxidation over palladium depends on the size of the metal crystallites and possibly on the distribution of sites on the metal surfaces.

The properties of samples 8 and 9 appear to be anomalous. These catalysts initially contain small particles, the linear-to-bridge peak ratios after reaction are near 1.0, yet the turnover frequencies are high. However, as described above, the infrared spectra of adsorbed carbon monoxide evidence a redistribution of sites on these catalysts during reaction. The new sites formed may be responsible for the high activities observed.

DISCUSSION

Comparison with the Literature

In Table 6, the results obtained in this study are compared with previously published work. Rates were extrapolated to our

TABLE 6

Comparison of Methane Oxidation Rates over Platinum and Palladium Measured in Different Laboratories

Reference	Reactor type	Catalyst composition	Turnover frequency (s^{-1})[a]		Activation energy (kcal/mole)[b]	
			Low	High	Low	High
This work	Continuous	Pt/Al_2O_3, ZrO_2	0.001	0.11	26.6	39.3
Anderson *et al.* (*10*)	Pulsed CH_4 in O_2	Pt/Al_2O_3	0.006	0.18	23.5	24.6
Yao (*14*)	Continuous	Pt/Al_2O_3	0.005	—	24.0	—
Niwa *et al.* (*16*)	Continuous	Pt/Al_2O_3, SiO_2, SiO_2–Al_2O_3	0.001	0.02	13.1	33.3
This work	Continuous	Pd/Al_2O_3, ZrO_2	0.02	5.6	25.7	30.1
Anderson *et al.* (*10*)	Pulsed CH_4 in O_2	Pd/Al_2O_3	—	0.9	—	21.8
Yao (*14*)	Continuous	Pd/Al_2O_3	0.05	1.4	17.0	20.0
Cullis and Willatt (*15*)	Pulsed CH_4/O_2 in He	Pd/Al_2O_3, TiO_2	18	43	17.9	22.7

[a] Turnover frequencies extrapolated to 335°C, 50 Torr CH_4 and 110 Torr O_2, using rate laws reported in the literature (*14–16*).

[b] 1 kcal = 4.184 kJ.

reaction conditions, using the reported activation energies and assuming, in all cases except Yao's platinum catalyst, that the rate is first order in methane pressure and zero order in oxygen pressure (*15*, *16*). In the case of Yao's platinum catalyst, the dependencies on methane and oxygen pressures were determined to be 0.7 and −0.6, respectively (*14*). Anderson and co-workers (*10*) did not measure the metal dispersion. However, to get a rough estimate of the turnover frequencies, a value of 10% was assumed for their catalysts. Cullis and Willatt (*15*) did not measure the metal dispersion either, but they did obtain transmission electron micrographs of the catalysts. The pictures indicate that the average metal particle varies from 11 to 26 nm in diameter. A dispersion between 3 and 9% is consistent with the particle diameters they observed (*18*). Both Anderson *et al.* and Cullis and Willatt obtained reaction rates in a transient mode, in which the reaction mixture was periodically pulsed over the catalyst. In our work, in Yao's, and in Niwa *et al.*'s rates were obtained during continuous operation.

Except for the results of Cullis and Willatt (*15*), the data obtained in the different laboratories are in good agreement. It is particularly noteworthy that we, Anderson *et al.* (*10*), Yao (*14*), and Niwa *et al.* (*16*) observe similar wide variations in the turnover frequencies for methane oxidation over the platinum and palladium catalysts. The unusually high rates measured by Cullis and Willatt may be due to testing the catalysts with stoichiometric mixtures of methane and oxygen (O_2/CH_4 = 2). The other three studies tested the catalysts in excess oxygen. Alternatively, the high rates may be a result of grossly underestimating the metal dispersion on these catalysts.

Structure Sensitivity of Platinum

Examination of the data in Table 3 reveals that methane oxidation over platinum is a structure-sensitive reaction. The turnover frequency changes by 100-fold from the least active to the most active catalyst. There is a strong correlation of turnover frequencies with the infrared spectrum of adsorbed carbon monoxide. Low turnover frequencies correspond to a broad band located at 2068 cm^{-1}, while high turnover frequencies correspond to a narrow band located at 2080 cm^{-1}. We now consider what

surface structures are implied by these characteristic absorbances.

Greenler, Hayden, and co-workers (*27–29*) obtained infrared spectra of carbon monoxide adsorbed on stepped platinum (111) single crystals at 85K. They observed two infrared peaks corresponding to adsorption at the steps and the terraces. The peaks shifted from 2065 to 2075 cm^{-1} and from 2085 to 2095 cm^{-1}, respectively, with increasing coverage. Their results suggest that the infrared bands observed on supported platinum catalysts may be due to carbon monoxide adsorption on the corner, edge, and close-packed face atoms of the crystallites (*28*). Corner and edge adsorption would give the band below 2075 cm^{-1}, while face adsorption would give the band above 2085 cm^{-1}.

The Greenler *et al.* model, however, is inconsistent with other experimental results. First, on supported platinum particles the low- and high-frequency bands, if they appear together in the spectrum, are observed at all coverages (*28*). Whereas on the stepped single-crystal surface, the dipoles of the face- and edge-bound carbon monoxide couple at high coverage and eliminate the low-frequency band (*27, 29*). Second, on our catalysts there is no correlation of peak type with particle size. For example, the platinum on sample 4 is completely dispersed, yet this sample exhibits a narrow infrared absorbance at 2083 cm^{-1}. It is difficult to rationalize how such highly dispersed platinum could also expose extended crystal faces of (111) orientation.

An alternative interpretation of the infrared spectra, proposed by Rothschild *et al.* (*30*), is that two phases of platinum coexist on the catalyst supports: a highly dispersed phase which is stabilized by alumina, and a crystalline phase which interacts only weakly with the support. Carbon monoxide adsorption on the dispersed phase is responsible for the 2068 cm^{-1} peak, while carbon monoxide adsorption on the crystalline phase is responsible for the 2080 cm^{-1} peak. These assignments are consistent with the single-crystal results. The vibrational frequency of carbon monoxide adsorbed on platinum in the dispersed phase is close to that for the low coverage limit of carbon monoxide adsorbed on stepped platinum (533) (*27*). This makes sense, since in both situations the adsorbed molecule is isolated. Furthermore, high carbon monoxide coverages on small platinum crystals should be analogous to islands of carbon monoxide on platinum (111). Depending on the size of the islands on Pt(111), the infrared absorbance shifts from 2085 to 2100 cm^{-1} (*26, 27*). This is in agreement with the position of the high-frequency band observed here and in other studies of supported platinum (*28, 30, 31*).

The presence of two phases of platinum on alumina has been established in several studies (*32* and references therein). The relative amount of the two phases formed depends on the support composition, the metal salt used, the amount of metal deposited, and the conditions of oxidation and reduction of the catalyst. High concentrations of the dispersed phase on alumina, up to 4 wt% platinum, can be obtained by adsorption of $PtCl_6^{2-}$, followed by oxidation between 300 and 500°C and reduction at 300° (*32*). Oxidation at 500°C produces a "platinum oxychloride" species (*33*). Oxidation at 700°C and above causes the oxychloride species to decompose into large platinum crystallites, although a small amount of the dispersed phase remains after this treatment (*30, 33*).

Our results show a similar relationship between preparation conditions and formation of the dispersed and crystalline phases of platinum. Three of the catalyst samples, 1, 3a, and 3b, were prepared by ion exchange of chloroplatinic acid onto alumina. Samples 1 and 3a were oxidized at 500°C and contain highly dispersed platinum. As expected, the infrared spectra of these samples are dominated by the peak at 2068 cm^{-1} (see Figs. 1 and 2). Sample 3b was oxidized at 700°C and contains large crystallites with a low dispersion. The infrared

spectrum for this sample at first seems anomalous because it exhibits a broad band centered at low wavenumbers. However, the crystallites on this sample may be extremely large (*30*), such that the inventory of surface platinum atoms on the crystallites is actually less than that on the small amount of dispersed phase remaining. Samples 4 and 5 utilized zirconia supports which do not stabilize the dispersed phase of platinum. Both of these samples show narrow infrared bands at 2080 cm^{-1}. Sample 2 was prepared in a way that should avoid formation of a dispersed phase. It was obtained by depositing the platinum amine complex onto a relatively inert alumina (α-AlOOH calcined at 1050°C for 2 h). As shown in Fig. 1, sample 2 exhibits the narrow, high-frequency band characteristic of adsorption on platinum crystallites.

Primet *et al.* (*31, 34*) and Peri (*35*) have shown that adsorption of other molecules with the carbon monoxide can shift the C–O stretching frequency up or down, depending on whether the coadsorbed molecule is an electron acceptor or electron donor. The infrared spectra shown in Figs. 1 and 2 are not affected by coadsorbed species, such as oxygen and chlorine, because these are removed from the surface by reduction at 300°C (*34, 35*).

In summary, the rate of methane oxidation is affected by the structure of the exposed platinum. Dispersed phase platinum is characterized by a broad infrared band at 2068 cm^{-1} for adsorbed carbon monoxide. It catalyzes the reaction at a turnover rate of 0.001 to 0.01 s^{-1} at 335°C with an apparent activation energy of 33 to 39 kcal/mole. Conversely, crystalline platinum is characterized by a narrow infrared band at 2080 cm^{-1} for adsorbed carbon monoxide. The crystallites catalyze the reaction at a turnover rate of 0.05 to 0.11 s^{-1} at 335°C with an apparent activation energy of 28 kcal/mole.

Structure Sensitivity of Palladium

Comparison of the data in Table 5 reveals that methane oxidation over palladium is a structure-sensitive reaction. The turnover frequency varies by a factor of 280 from the least active to the most active catalyst. The turnover frequencies depend strongly on the size of the palladium particles. Samples 11b, 12a, and 12b, with greater than 35% dispersion, are much less active than samples 10, 13b, and 14, with less than 12% dispersion. Samples 8 and 9 were unstable during reaction, so their behavior is considered separately below.

For samples 10, 11b, 12a, 12b, 13b, and 14, the infrared spectra of adsorbed carbon monoxide show a decrease in the linear-to-bridge peak ratio with increasing particle size. This trend is consistent with the types of surface sites assigned to these peaks. The band due to bridge-bonded carbon monoxide has been attributed by many authors to adsorption on the faces of the small palladium crystals (*22, 24, 25, 36, 37*). On the other hand, the band due to linearly bonded carbon monoxide has been attributed to adsorption on all types of sites (*22*), including single-crystal planes (*25*) and isolated atoms (*38*). Thus, on small crystallites with a high fraction of corner and edge atoms, the ratio of linearly bonded to bridge-bonded carbon monoxide should be relatively high; while on large crystallites with a high fraction of face atoms, the ratio of linearly bonded to bridge-bonded carbon monoxide should be relatively low. This is in agreement with the data reported in Table 5.

For samples 8 and 9, the infrared spectra recorded before and after reaction evidence a dramatic change in the structure of the palladium crystallites. The before and after spectra are shown in Fig. 4. As a result of exposure to reaction conditions, the linear-to-bridge peak ratio decreases by a large amount, and is accompanied by growth of the 1970 cm^{-1} band. The 1970 cm^{-1} band has been attributed to carbon monoxide adsorption on (100) planes (*22, 24, 25, 36, 37*). The shift in the distribution of the infrared bands is therefore consistent with an agglomeration of the palladium crystallites during reaction. The dispersion during

steady state reaction is probably much lower than that given in Table 5, and brings the results obtained for samples 8 and 9 into line with those for samples 10, 13b, and 14.

The size of the palladium crystallites which could be stabilized on the supports depended on the support composition and method of preparation. Small crystallites were produced by ion exchanging a small amount of palladium, less than 0.5 wt%, onto the high-surface-area Degussa alumina. Large crystallites were produced by depositing either a large amount of palladium. 2.3 wt%, on the Degussa alumina or by depositing the palladium on the other lower-surface-area alumina and zirconia supports.

Possible Explanation of the Structure Sensitivity

Under our reaction conditions, the exposed platinum and palladium surfaces are covered with oxygen. This conclusion is supported by several facts: (1) In most cases, the observed rate law is first order in methane pressure and zero order in oxygen pressure (*11–16*). (2) Oxygen adsorption on platinum and palladium is extremely fast and irreversible below 400°C (*39*). Methane adsorption, on the other hand, is a slow, activated process (*40*). Oxygen should completely displace methane from the surface when the O_2/CH_4 ratio exceeds 2. Therefore, the structure sensitivity of methane oxidation should be related to differences in the reactivity of the adsorbed oxygen.

The interaction of oxygen with supported platinum catalysts has been investigated in several laboratories (*15, 16, 33, 41, 42*). When platinum is completely dispersed, it oxidizes to PtO_2 starting at 300°C (*33, 41, 42*). However, when platinum is in the form of crystallites, only the surfaces of the crystallites are oxidized during heating in air up to 600°C (*15, 33, 41*). This is so irrespective of their size (*42*). If chlorine is present, the crystalline phase oxidizes more readily, and complete oxidation of the platinum has been observed at 500°C (*16, 32*). The dispersed PtO_2 is less reactive toward hydrogen than the surface oxygen on the platinum crystallites (*32, 41*). Temperature-programmed reduction (TPR) of catalysts previously oxidized at 300°C produces a broad, high-temperature peak corresponding to the dispersed phase, and a narrow, low-temperature peak corresponding to the crystalline phase (*41*). The high reactivity of the oxygen on the crystallites suggests that it is a "chemisorbed layer" and not a "surface oxide."

The rate of methane oxidation is expected to follow the rate of hydrogen reduction of the oxygen covered platinum. Both of these reactions proceed by the rate limiting adsorption of the reducing reactant onto the surface oxygen (*14, 15*). Both reactions exhibit the same kinetics: first order in reducing reactant and zero order in oxygen (*43*). The observation of separate temperature maxima in the TPR traces of platinum catalysts indicates that the activation energies for reduction of each type of surface oxygen are different. More specifically, the activation energy of hydrogen reaction with dispersed PtO_2 is higher than that with adsorbed oxygen on Pt crystallites. In agreement with these findings, we observe a higher activation energy for methane oxidation on the dispersed phase than on the crystalline phase (compare the activation energies of samples 1 and 2 in Table 3).

Niwa *et al.* (*16*) observed a correlation of the rates of methane oxidation with the temperature-programmed reduction of platinum catalysts. A broad, low-temperature peak in the TPR trace corresponded to reduction of the adsorbed oxygen. This peak shifted upward in temperature along with a decrease in the turnover frequency and an increase in the activation energy for methane oxidation. The results of Niwa *et al.* are consistent with the existence of two types of surface oxygen, each with different reactivities toward hydrogen and methane.

Studies of platinum single crystals have shown that oxygen reacts with at most the top two layers of the surface over a wide range of temperatures and oxygen pres-

sures (*44, 45*). Below 500°C, oxygen dissociatively chemisorbs onto the surface of the platinum crystals. At higher temperatures, an unreactive surface oxide may form. Gland (*46*) conducted a comprehensive study of oxygen adsorption on flat and stepped Pt(111). He observed almost no difference in the energy of adsorption between the flat and the stepped surfaces. This result is pertinent to supported platinum catalysts, because it suggests that the reactivity of oxygen adsorbed on corner, edge, and face atoms of crystallites should be the same. In other words, the reactivity of the adsorbed oxygen should not change with crystallite size. Returning our attention to the TPR results, the observation by McCabe and co-workers (*41*) of a separate high-temperature peak on the more highly dispersed platinum catalysts is inconsistent with a simple change in the diameter of the metal particles. Rather there is a less reactive dispersed PtO_2 and a more reactive oxygen adsorbed on Pt crystallites; the latter decreases in concentration relative to the former as the dispersion of the platinum increases.

The interaction of oxygen with palladium catalysts differs from that observed for platinum catalysts. Between 200 and 900°C in an oxidizing environment, some fraction of the interior of the palladium particles oxidizes (*47*). Oxidation breaks apart the metal crystallites, so that all the oxide formed is exposed and participates in catalysis (*19*). Under our reaction conditions of 260 to 350°C and excess oxygen, some of the bulk palladium oxidizes, causing an increase in the number of active sites. Consequently, it is incorrect to base the turnover frequencies on the initial dispersion as has been done in Tables 4–6. However, at the time these measurements were taken, we did not know that the number of surface palladium atoms increases during reaction, and adsorption measurements were not made on the used samples. Thus, to provide a comparison of the platinum and palladium catalysts tested in this and in previous studies, initial dispersions were used to calculate the turnover frequencies.

In the accompanying paper (*19*), we show that the extent of palladium oxidation depends on the metal particle size. At 300°C and 110 Torr of oxygen, small crystallites are completely oxidized, while large crystallites are partially oxidized. The completely oxidized palladium disperses over the alumina as PdO. The partially oxidized palladium is broken into smaller crystallites which are covered with a layer of oxygen. A rough estimate of the turnover frequencies, corrected for palladium oxidation, can be made by assuming that the dispersion is 1.0 for small particles (samples 11b and 12b) and 0.5 for large particles (samples 8, 9, 10, 13b, and 14) (*19*). The recalculated turnover frequencies are 0.02 s^{-1} for the former and from 0.7 to 3.0 s^{-1} for the latter. These results suggest that the palladium oxide dispersed over the alumina is much less active than the oxide covering the fcc palladium crystallites (*19*). This interpretation is analogous to what we have observed for platinum.

In summary, the structure sensitivity of platinum and palladium for methane oxidation may be explained by the different reactivities of adsorbed oxygen. The results suggest that there are four types of surface oxide: platinum oxide dispersed over alumina, oxygen adsorbed on platinum crystallites, palladium oxide dispersed over alumina, and oxygen adsorbed on palladium crystallites. At 335°C, the turnover rates for methane oxidation increase as follows: dispersed PtO_2, TOF = 0.005 s^{-1}; dispersed PdO, TOF = 0.02 s^{-1}; Pt crystallites, TOF = 0.08 s^{-1}; and Pd crystallites, TOF = 1.3 s^{-1}.

The possibility that residual chlorine on the catalyst poisons the reaction should be considered. We suspect that samples 3a and 12a may be affected by chloride poisoning. Both of these catalysts were prepared by ion exchange of the metal chloride with Degussa alumina. Both of these catalysts exhibited reaction rates which steadily in-

creased throughout the run, as if a poison was slowly being removed from the metal particles. No effect of chlorine is apparent in the infrared spectrum of adsorbed carbon monoxide on these samples. However, in the accompanying paper (*19*), we show that palladium on Degussa alumina, prepared by ion exchange of H_2PdCl_4, oxidation at 500°C, and reduction at 300°C, shows abnormal methane and oxygen adsorption characteristics. Palladium on alumina oxidized at higher temperatures does not exhibit this behavior.

CONCLUSIONS

We have measured the intrinsic rates of methane oxidation in 5% excess oxygen over a series of platinum and palladium catalysts. The steady state turnover frequencies vary over a wide range, depending on the structure of the metal surface. Two types of platinum are present, a dispersed phase and a crystalline phase. The two phases are identified by their characteristic infrared spectra for adsorbed carbon monoxide. The former exhibits a 42 cm^{-1} wide band at 2068 cm^{-1}, while the latter exhibits a 23 cm^{-1} wide band at 2080 cm^{-1}. Under reaction conditions, the dispersed phase is converted into PtO_2 while the crystallites are covered with adsorbed oxygen. The methane oxidation activity of the dispersed PtO_2 is 10 to 100 times lower than that of the platinum crystallites. Whether or not the dispersed or crystalline phases are formed depends more on the support composition and the method of preparation, than on the degree to which the platinum is dispersed over the support.

Over palladium, the turnover frequency for methane oxidation depends on particle size. Under reaction conditions, small crystallites on alumina are converted into dispersed PdO, while large crystallites are converted into smaller ones covered with adsorbed oxygen (*19*). The results suggest that the methane oxidation activity of the dispersed PdO is 10 to 100 times lower than that of the small palladium crystallites.

ACKNOWLEDGMENT

This work was supported by the Gas Research Institute through Contract 5086-260-1247.

REFERENCES

1. Prasad, R., Kennedy, L. A., and Ruckenstein, E., *Catal. Rev. Sci. Eng.* **26,** 1 (1984).
2. Kesselring, J. P., *in* "Advanced Combustion Methods" (F. J. Weinberg, Ed.), p. 237. Academic Press, New York, 1986.
3. Pfefferle, L. D., and Pfefferle, W. C., *Catal. Rev. Sci. Eng.* **29,** 219 (1987).
4. Trimm, D. L., and Lam, C. W., *Chem. Eng. Sci.* **35,** 1405 (1980).
5. Machida, M., Eguchi, K., and Arai, H., *J. Catal.* **103,** 385 (1987).
6. Wei, J., *Adv. Catal.* **24,** 57 (1975).
7. Kim, G., *Ind. Eng. Chem. Prod. Res. Dev.* **21,** 267 (1982).
8. Spivey, J. J., *Ind. Eng. Chem. Res.* **26,** 2165 (1987).
9. Gandhi, H. S., and Shelef, M., *in* "Atmospheric Ozone Research and Its Policy Implications" (T. Schneider, Ed.), p. 1037. Elsevier, Amsterdam, 1989.
10. Anderson, R. B., Stein, K. C., Feenan, J. J., and Hofer, L. J. E., *Ind. Eng. Chem.* **53,** 809 (1961).
11. Mezaki, R., and Watson, C. C., *Ind. End. Chem. Process Des. Dev.* **5,** 62 (1966).
12. Firth, J. G., and Holland, H. B., *Nature (London)* **217,** 1252 (1968).
13. Firth, J. G., and Holland, H. B., *Trans. Faraday Soc.* **65,** 1121 (1969).
14. Yao, Y. F. Y., *Ind. Eng. Chem. Prod. Res. Dev.* **19,** 293 (1980).
15. Cullis, C. F., and Willatt, B. M., *J. Catal.* **83,** 267 (1983).
16. Niwa, M., Awano, K., and Murakami, Y., *Appl. Catal.* **7,** 317 (1983).
17. Seimanides, S., and Stoukides, M., *J. Catal.* **98,** 540 (1986).
18. Van Hardeveld, R., and Hartog, F., *Surf. Sci.* **15,** 189 (1969).
19. Hicks, R. F., Young, M. L., Lee, R. G., and Qi, H., *J. Catal.* **122,** 294 (1990).
20. Anderson, J. R., "Structure of Metallic Catalysts." Academic Press, New York, 1975.
21. Benson, J. E., and Boudart, M., *J. Catal.* **4,** 704 (1965).
22. Hicks, R. F., Yen, Q. J., and Bell, A. T., *J. Catal.* **89,** 498 (1984).
23. Eischens, R. P., and Pliskin, W. A., *Adv. Catal.* **10,** 1 (1958).
24. Sheppard, N., and Nguyen, T. T., *in* "Advances in Infrared and Raman Spectroscopy" (R. J. H. Clark and R. E. Hester, Eds.), p. 67. Heyden & Sons, Ltd., London, 1978.

25. Hoffmann, F. M., *Surf. Sci. Rep.* **3,** 107 (1983).
26. Bradshaw, A. M., and Schweizer, E., *in* "Advances in Spectroscopy: Spectroscopy of Surfaces" (R. J. H. Clark and R. E. Hester, Eds.), p. 413. Wiley, New York, 1988.
27. Hayden, B. E., Kretzschmar, K., Bradshaw, A. M., and Greenler, R. G., *Surf. Sci.* **149,** 394 (1985).
28. Greenler, R. G., Burch, K. D., Kretzschmar, K., Klauser, R., Bradshaw, A. M., and Hayden, B. E., *Surf. Sci.* **152/153,** 338 (1985).
29. Leibsle, F. M., Sorbello, R. S., and Greenler, R. G., *Surf. Sci.* **179,** 101 (1987).
30. Rothschild, W. G., Yao, H. C., and Plummer, H. K., *Langmuir* **2,** 588 (1986).
31. Primet, M., *J. Catal.* **88,** 273 (1984).
32. Yao, H. C., Sieg, M., and Plummer, H. K., *J. Catal.* **59,** 365 (1979).
33. Lieske, H., Lietz, G., Spindler, H., and Volter, J., *J. Catal.* **81,** 8 (1983).
34. Primet, M., Basset, J. M., Mathieu, M. V., and Prettre, M., *J. Catal.* **29,** 213 (1973).
35. Peri, J. B., *J. Catal.* **52,** 144 (1978).
36. Palazov, A., Kadinov, G., Bonev, Ch., and Shopov, D., *J. Catal.* **74,** 44 (1982).
37. Beebe, T. P., and Yates, J. T., *Surf. Sci.* **173,** L606 (1986).
38. Clarke, J. K. A., Farren, G., and Rubalcava, H. E., *J. Phys. Chem.* **71,** 2376 (1967).
39. Engel, T., and Ertl, G., *Adv. Catal.* **28,** 1 (1979).
40. Frennet, A., *Catal. Rev. Sci. Eng.* **10,** 37 (1974).
41. McCabe, R. W., Wong, C., and Woo, H. S., *J. Catal.* **114,** 354 (1988).
42. Nandi, R. K., Molinaro, F., Tang, C., Cohen, J. B., Butt, J. B., and Burwell, R. L., *J. Catal.* **78,** 289 (1982).
43. Boudart, M., and Djega-Mariadassou, G., "Kinetics of Heterogeneous Catalytic Reactions," p. 172. Princeton Univ. Press, Princeton, NJ, 1984.
44. Ducros, R., and Merrill, R. P., *Surf. Sci.* **55,** 227 (1976).
45. Matsushima, T., Almy, D. B., and White, J. M., *Surf. Sci.* **67,** 89 (1977).
46. Gland, J. L., *Surf. Sci.* **93,** 487 (1980).
47. Bayer, G., and Wiedemann, H. G., *Thermochim. Acta* **11,** 79 (1975).